HHS Public Access

Author manuscript

Dalton Trans. Author manuscript; available in PMC 2019 March 12.

Published in final edited form as:

Dalton Trans. 2018 March 12; 47(11): 3733–3738. doi:10.1039/c8dt00058a.

Expanding the allyl analogy: accessing η^3-*P,B,P* diphosphinoborane complexes of group 10†

Marcus W. Drover and **Jonas C. Peters***

Division of Chemistry and Chemical Engineering, California Institute of Technology, Pasadena, California, 91125, USA

Abstract

Using the diphosphinoborane, $(PPh_2)_2BMes$ (Mes = 2,4,6-$Me_3C_6H_3$), we report the first examples of η^3-*P,B,P*-ligated complexes using Ni(0) and Pt(II). Reaction of $(PPh_2)_2BMes$ with $Ni(COD)_2$ or $Pt(COD)Me_2$ (COD = 1,5-cyclooctadiene) results in gradual COD displacement to give [η^3-*P,B,P*-$(PPh_2)_2BMes$]Ni(COD) (**3**) or [η^3-*P,B,P*-$(PPh_2)_2BMes$]$Pt(CH_3)_2$ (**6**). Complex **3** serves as a versatile Ni-containing synthon for the preparation of square planar or tetrahedral Ni(0) complexes. Notably, the M–B interaction in these systems is non-negligible – with coordination resulting in an upfield shift of *ca.* 80 ppm in the ^{11}B NMR spectrum. We also show that treatment of the Pt^{IV} halide precursor, $[PtMe_3I]_4$ with this ligand framework results in migration of X-type ligands (CH_3^- and I^-) to boron and reductive elimination of ethane (C_2H_6) to give a distorted square planar zwitterionic Pt^{II} complex, Pt[κ^2-*P,P*-$(PPh_2)_2B(Mes)(CH_3)$][κ^2-*P,P*-$(PPh_2)_2B$ (Mes)(I)] (**10**). This reactivity suggests the feasibility of $(PPh_2)_2BMes$-ligand-induced labilization of M–X ligands.

Introduction

Allyl ligands $[C_3H_5]^-$ represent a cornerstone of organometallic chemistry, stabilizing transition and main group elements in a η^1- or η^3-bonding fashion. Drawing inspiration from the 'all-carbon'-based allyl fragment, related ligands have emerged incorporating a *Z*-type[1] accepting boron atom *in lieu* of carbon. Shapiro and co-workers, for example, reported that the zwitter-ionic bis(triphenylphosphinemethylenido)borane ligand coordinates in an η^3-*C,B,C* fashion to both Zr(IV) and Pd(II) (Chart 1A).[2] By analogy, Emslie and co-workers found that vinylboranes ($R_2C{=}CR{-}BR_2$) serve as precursors to η^3-*B,C,C* coordinated complexes of Ni(0) and Pt(0) adopting borataallyl coordination modes (Chart 1A).[3] In a similar vein, our group and others have characterized related η^3-*B,C,C* complexes using (phosphine)borane-based ligand platforms, where the metal centre engages in bonding with both boron and a π-acidic aryl ring.[4–6] Building on our group's previous efforts in *P,B*-containing coordination complexes of late transition metals, we wished to explore direct P–

†Electronic supplementary information (ESI) available: ^1H, ^{31}P, ^{11}B, and ^{13}C NMR spectra for all complexes as well as crystallographic data for 2, 3, 5, 6, and 10. CCDC 1581574–1581579 contains the supplementary crystallographic data for this paper. For ESI and crystallographic data in CIF or other electronic format see DOI: 10.1039/c8dt00058a

* jpeters@caltech.edu.

Conflicts of interest

There are no conflicts to declare.

B linkages as isolobal fragments to C=C bonds *e.g.*, $[R_2C{=}CR{-}CR_2]^-$ *vs.* $R_2P{=}B(R){-}PR_2$. This approach has been highlighted by isolation of the η^6-*P*$_3$,*B*$_3$-containing arene complex $[\{\eta^6\text{-}[(P^tBu)(BMes)]_3\}Cr(CO)_3]$7 and the η^2-*P,B* phosphinoborane complexes, $Pt(PPh_3)_2(\eta^2\text{-}R_2P{=}B(C_6F_5)_2)$ (R = Cy or *t*Bu), providing evidence for alkene-type coordination of P=B multiple bonds (Chart 1B).[8] We now disclose that the diphosphinoborane, $(PPh_2)_2BMes$ (**1**: Mes = 2,4,6-$Me_3C_6H_3$) first prepared by Power and co-workers,[9] serves as a practical starting point from which η^3-*P,B,P* bonded complexes of group 10 transition metals can be accessed.

Generation of $[\eta^3\text{-}P,B,P\text{-}(PPh_2)_2BMes]Ni(COD)$ (**2**; COD = 1,5-cyclooctadiene) was achieved by combination of $(PPh_2)_2BMes$ with $Ni(COD)_2$ in benzene at ambient temperature, which provides a dark brown solution (Scheme 1). Monitoring the reaction by ^1H NMR spectroscopy evidences loss of cyclooctadiene (C_6D_6: δ_H = 5.58 and 2.21 ppm) and formation of a new C_s-symmetric Ni(0) complex. Notably, three unique mesityl $-CH_3$ signals are observed (each of integration 3H) at δ = 2.58, 2.13, and 1.30 ppm, indicative of both (1) hindered B–C bond rotation and (2) the absence of a B–Ni decoordination/recoordination process (where the boron atom transiently dissociates only to reassociate on the opposite face of the molecule). Further, by ^1H NMR spectroscopy, coalescence of the *ortho*-CH_3(mesityl) groups is not observed at elevated temperature (95 °C, tol-d_8). It is noteworthy that this phenomenon is observed for all η^3-*P,B,P*-$(PPh_2)_2BMes$ complexes discussed herein. A strong Ni–B interaction is corroborated by ^{11}B NMR spectroscopy [δ_B = +4.0; Δδ = −81.0 *cf.* **1**] (Fig. 1), while ^{31}P NMR spectroscopy provides a new signal at δ_P = −16.6 (Δδ = −16.5 *cf.* **1**) – coupling between ^{11}B and ^{31}P is not observed. High-resolution FAB-MS also provides a $[M]^+$ signal consistent with the molecular formula of **2** at *m*/*z* = 666.229 (calcd 666.229).

Orange/brown crystals of **2** can be obtained from a saturated Et_2O solution at −35 °C allowing for unambiguous structural determination using single crystal X-ray diffraction (Fig. 2). Complex **2** crystallizes in the triclinic space group, $P\bar{1}$ and features a tetrahedral Ni(0) complex bonded to PBP and COD co-ligands having Ni(1)–P(1) and Ni(1)–P(2) bond lengths of 2.183(1) and 2.190(1) Å and a Ni(1)–B(1) bond distance of 2.329(4) Å. This distance is considerably shorter than that noted for a related compound, $[(Ph_3P)_2Ni(\eta^3\text{-}B,C,C\text{-}VB^{Ph})]$ (VB^{Ph} = (*E*)-PhHC=CH–$B(C_6F_5)_2$ (d_{Ni-B} = 2.660(3) Å)).[3] The boron centre also retains sp^2-hybridization [∑(X–B–X) = 360°] and upon coordination, little perturbation in P–B bond length is noted [1.888(4)/1.907(4) Å *cf.* 1.879(2)/1.901(2) Å for **1**]. Consistent with increased planarization, the sum of angles at phosphorus, [∑(X–P–X) = 340.2° and 342.7°] also increase by *ca.* 20° [318.8° and 324.5° for **1**]. These data indicate that coordination of **1** involves some degree of P–B–P communication/π-orbital overlap, signifying that the ligand is electronically distinct from its relative, bis(diphenylphosphino) methane (dppm). Highlighting the electrophilic nature of boron in this family of compounds, treatment of **1** with $NiCl_2$ or $NiBr_2$(dme) (dme = 1,2-dimethoxyethane) in THF or Et_2O leads to rapid B–P bond rupture, forming the known tetrahedral Ni(0)-species, $Ni(PPh_2H)_4$[10] and $MesBX_2$ (X = Cl, Br). We posit that the H-atoms in $Ni(PPh_2H)_4$[10] arise from radical H-atom transfer (HAT), presumably from solvent.

To evaluate the effect of co-ligand on η^3-*P,B,P* bonding and to further study the nature of the Ni–B interaction, we next ventured to treat complex **2** with L-type ligands. Dissolution of complex **2** in coordinating solvents: MeCN-d_3, pyridine-d_5, or THF-d_8 did not result in Ni–B dissociation as judged by ^{11}B and ^{31}P NMR spectroscopy. Conversely, treatment of a benzene solution of complex **2** with 2,2′-bipyridine (2,2′-bpy) slowly (4 days) produces a dark purple solution, identified as the tetrahedral Ni(0) complex, [η^3-*P,B,P*-$(PPh_2)_2$BMes]Ni(2,2′-bpy) (**3**) along with free COD (Scheme 1). This complex displays two deshielded resonances in the ^{1}H NMR spectrum at δ = 9.92 and 8.92 ppm for each of its two *ortho*-CH pyridyl groups, indicating C_s-symmetry. Further, ^{11}B NMR spectroscopy supports a maintained interaction between Ni and B [δ_B = −7.7], while ^{31}P NMR spectroscopy provides a new signal at δ_P = −20.9. Purple blocks, suitable for X-ray analysis were obtained from a concentrated THF/pentane solution at −35 °C (Fig. 3). Complex **3** possesses similar Ni(1)–P(1) and Ni(1)–P(2) bond lengths to complex **2** of 2.1625(6) and 2.1751(9) Å, albeit a shorter Ni(1)–B(1) bond length of 2.201(3) Å. For the 2,2′-bpy ligand, all bond lengths are consistent with redox innocence.[11]

By analogy, the COD ligand of complex **2** is readily displaced by the π-accepting ligands 2,6-dimethylphenylisonitrile (CNXyl) or diphenylacetylene to give complexes **4** and **5**, respectively (Scheme 1). For the bis(CNXyl) analogue **4** a single ^{11}B and ^{31}P NMR resonance at δ_B = +4.8 ppm and δ_P = −8.5 ppm is observed. Three broad signals are observed by IR spectroscopy at ν(*CN*) = 2078, 2039, and 1993 cm^{-1} (*cf.* 2123 cm^{-1} for free CNXyl), again indicating moderate π-back donation. Over a period of hours complex **4** decomposes in solution to as yet unidentified species, obviating analysis by X-ray crystallography. For the square planar complex **5**, NMR spectroscopy supports the formation of a C_s-symmetric complex (δ_B = +6.7 ppm and δ_P = −8.1 ppm) and the IR spectrum exhibits a feature at 1823 cm^{-1} (consistent with π-back donation by η^3-*P,B,P*-Ni^0). The solid-state structure of complex **5** was also obtained (Fig. 3). By contrast to complexes **2** and **3**, for complex **5**, Ni(1)–P(1) and Ni(1)–P(2) bonds of 2.2040(7) and 2.1905(9) Å represent a slight elongation at the cost of the Ni(1)–B(1) bond [2.254(3) Å], which is slightly shortened. Complex **5** is structurally similar to the η^2-alkyne complex, reported by Hillhouse *et al.* [dtbpe]Ni(η^2-PhCuCPh) (dtbpe = 1,2-bis(di-*tert*-butyl)phosphinoethane) for which ν(*CC*) = 1790 cm^{-1}.[12]

Expansion of the ligand platform to Pt^{II} was also established. Combination of **1** and $Pt(Me)_2$(COD) in benzene at ambient temperature provides a light yellow solution over a period of four days (Scheme 2). NMR spectroscopic analysis of a C_6D_6 solution of this mixture provides evidence for two Pt-containing species in a 9: 1 ratio: [η^3-*P,B,P*-$(PPh_2)_2$BMes] $Pt(Me)_2$ (**6**) and the known complex, $Pt(PHPh_2)_2(Me)_2$.[13] Complex **6** could be purified and separated by recrystallization from Et_2O at −35 °C in 88% yield. By analogy to complex **2**, the ^{1}H NMR spectrum of **6** features three diagnostic signals, each of integration of 3H at δ = 2.81, 2.78, and 2.06 ppm for the mesityl group, while for the platinum-methyl groups, an apparent triplet is observed at δ = 2.18 ppm [$^3J_{Pt,H}$ = 80 Hz] that corresponds to δ_c = 4.52 ppm (t, $^2J_{C,P}$ = 27.8 Hz) with ^{195}Pt satellites ($^1J_{C,Pt}$ = 688 Hz) in the ^{13}C NMR spectrum. Coordination of Pt^{II} to the PBP unit is also evidenced by ^{31}P and

^{11}B NMR spectroscopy, which provides a signal at δ_P = −21.6 [$^1J_{Pt,P}$ = 839 Hz] and δ_B = +7.9 ppm [$\Delta\delta_B$= −77.1 *cf.* **1**].

The solid-state structure of complex **6** is depicted in Fig. 4. The four-coordinate geometry is best described as square planar, having Pt(1)–P(1) and Pt(1)–P(2) contacts of 2.305(3) and 2.318(2) Å and a Pt(1)–B(1) distance of 2.403(11) Å. The Pt(1)–C(1) and Pt(1)–C(2) bond lengths are non-exceptional.

Given the halophilic nature of **1**, we wondered if capture of an X-type ligand by B could be performed in a controlled manner – in effect promoting metal–ligand cooperativity.[14–19] As a result, **1** was treated with 0.25 equiv. of the Pt^{IV} precursor, $[PtMe_3I]_4$ resulting in slow effervescence of C_2H_6 [δ_H = 0.80 ppm] as judged by ^{1}H NMR spectroscopy. By ^{31}P NMR spectroscopy, consumption of the ligand and the appearance of a broad multiplet centred at δ_P = −35.7 was observed (see ESI, Fig. S28†) over a period of four days. Removal of volatiles *in vacuo* and recrystallization of the resulting solid from Et_2O at −35 °C, provided colourless prisms suitable for single crystal analysis. Analysis of the resulting crystal data provides evidence for Pt[κ^2-*P,P*-$(PPh_2)_2$B(Mes)(I)][κ^2-*P,P*-$(PPh_2)_2$B(Mes) (CH_3)] (**10**) (Fig. 5). Notably, the B–C$\underline{H}_3$ resonance for complex **10** appears as a phosphorus-coupled triplet at δ_H = 1.45 [$^3J_{P,H}$ = 19.4 Hz]. We posit that coordination of 'PtMe$_3$I' to **1** provides the octahedral Pt^{IV} complex **7**, which is susceptible to halide abstraction by **1**, providing the coordinatively unsaturated five-coordinate complex **8**. Reductive elimination of ethane (C_2H_6) from **8** thus provides complex **9**, which upon methyl abstraction by another equivalent of **1** gives complex **10**. Abstraction of X-type halide and methyl groups by group 13 Lewis acids is well documented.[20–24] The crystal structure of **10** features a distorted square planar Pt(II) centre (τ_4 = 0.23)[25] bonded by four phosphorus atoms. By contrast to complex **6**, each boron atom in the ligand is sp^3-hybridized in nature, owing to association of the X-type iodide or methyl anion causing the P–B bond lengths elongate: [2.036(4) and 2.064(4) Å *cf.* 1.85(1) and 1.89(1) Å for **6**].

Conclusion

In close, we have provided here the first examples of Ni^0 and Pt^{II} compounds containing a P–B–P diphosphinoborane ligand. This work expands the scope of P–B bond coordination complexes beyond that of the known η^6-PvB and η^2-PvB coordination modes and illustrates the use of diphosphinoboranes as modular η^3-*P,B,P* chelates.

Experimental section

General considerations

All experiments were carried out employing standard Schlenk techniques under an atmosphere of dry nitrogen or argon employing degassed, dried solvents in a solvent purification system supplied by SG Water, LLC. Combustion analyses were carried out by Midwest Microlabs (Indianapolis). N.B. The results provided represent the best analysis values obtained. Multinuclear NMR spectroscopy has been provided (see ESI†) to illustrate sample homogeneity. Non-halogenated solvents were tested with a standard purple solution of sodium benzophenone ketyl in tetrahydrofuran in order to confirm effective moisture

removal. $(PPh_2)_2BMes$[9] was prepared according to a literature procedure. All other reagents were purchased from commercial vendors and used without further purification unless otherwise stated.

Physical methods

Fourier transform infrared ATR (FT-IR ATR) spectra were collected on a Thermo Scientific Nicolet iS5 Spectrometer with diamond ATR crystal. NMR data were collected on a Varian 400 MHz instrument with chemical shifts reported in ppm relative to C_6D_6 or THF-d_8, using residual solvent resonances as internal standards. N.B. In some instances, not all aromatic carbon atoms are viewed due to overlap with residual C_6D_6. ^{31}P chemical shifts are reported in ppm relative to 85% aqueous H_3PO_4. $^{11}B\{^1H\}$ NMR spectra were acquired using quartz NMR tubes.

$(PPh_2)_2BMes$ (1)

This compound was prepared as previously, however the ^1H and ^{13}C NMR data were not provided.[9] Also, in our hands a $^{11}B\{^1H\}$ NMR chemical shift of 85.0 ppm was recorded in C_6D_6 or 1: 1 C_6D_6:THF, which is different from that reported (30.0 ppm). **^{1}H NMR (400 MHz, C_6D_6, 298 K):** δ = 7.29 (m, 8H; *o*-PPh_2), 6.90 (m, 8H; *m*-PPh_2), 6.89 (m, 4H; *p*-PPh_2), 6.69 (s, 2H; Mes), 2.20 (s, 3H; Mes), 2.18 (s, 6H; Mes). **$^{13}C\{^1H\}$ NMR (100 MHz, C_6D_6, 298 K):** δ = 137.61 (t, $J_{C,P}$ = 2.1 Hz), 137.28 (t, $J_{C,P}$ = 5.9 Hz), 134.61 (t, $J_{C,P}$ = 7.9 Hz), 134.19 (t, $J_{C,P}$ = 6.4 Hz), 128.42 (t, $J_{C,P}$ = 4.2 Hz), 128.00 (under C_6D_6), 127.92 (t, $J_{C,P}$ = 4.2 Hz), 22.51 (t, $J_{C,P}$ = 2.5 Hz), 21.38. **$^{31}P\{^1H\}$ NMR (161.9 MHz, C_6D_6, 298 K):** δ = −0.01. **$^{11}B\{^1H\}$ NMR (128 MHz, C_6D_6, 298 K):** δ = 85.0.

$[\eta^3$-*P,B,P*-$(PPh_2)_2BMes]Ni(COD)$ (2)

In the glovebox, **1** (45 mg, 0.090 mmol) and $Ni(COD)_2$ (25 mg, 0.091 mmol) were added to a 20 mL vial equipped with a stir bar. Approximately 2 mL of benzene was added and the orange solution was allowed to stir for 4 days at 25 °C. The solvent was removed *in vacuo* and the resulting orange oil was washed with pentane to afford an orange/brown solid. Recrystallization from saturated Et_2O at −35 °C gave orange crystals (56 mg, 93%). **^{1}H NMR (400 MHz, THF-d_8, 298 K):** δ = 7.40 (m, 4H; PPh_2), 7.08 (m, 12H; PPh_2), 6.89 (t, $^3J_{H,H}$ = 7.2 Hz, 4H; PPh_2), 6.66 (s, 1H; Mes), 6.44 (s, 1H; Mes), 5.09 (s, 2H; COD), 4.27 (s, 2H; COD), 2.83 (br, 2H; COD), 2.58 (s, 3H; Mes), 2.47 (br m, 4H; COD), 2.27 (br m, 2H; COD), 2.13 (s, 3H; Mes), 1.30 (s, 3H; Mes). **$^{13}C\{^1H\}$ NMR (100 MHz, C_6D_6, 298 K):** δ = 141.36, 139.78, 136.70 (t, $J_{C,P}$ = 33 Hz), 135.46, 134.86 (t, $J_{C,P}$ = 5.4 Hz), 133.74 (t, $J_{C,P}$ = 5.1 Hz), 132.05 (t, $J_{C,P}$ = 23 Hz), 128.40, 93.07, 87.63, 32.13, 31.06, 25.86, 23.26, 21.17. **$^{31}P\{^1H\}$ NMR (161.9 MHz, THF-d_8, 298 K):** δ = −16.6 (br). **$^{11}B\{^1H\}$ NMR (128 MHz, THF-d_8, 298 K):** δ = +4.03 (br). **FAB-MS (*m/z*):** 666.229 (calcd 666.229). **Anal. calcd** for $C_{41}H_{43}BNiP_2$ (666.23): C, 73.80; H, 6.50. Found: C, 72.20; H, 7.11.

$[\eta^3$-*P,B,P*-$(PPh_2)_2BMes]Ni(2,2'$-bipy) (3)

In the glovebox, **2** (30 mg, 0.045 mmol) and 2,2′-bipyridine (7.0 mg, 0.048 mmol) were added to a 20 mL vial equipped with a stir bar. Approximately 2 mL of benzene was added and the orange solution was allowed to stir for 4 days at 25 °C. The solvent was removed *in*

vacuo and the resulting purple oil was recrystallized from pentane at −35 °C to give purple crystals (14 mg, 44%) N.B. Low yields are due to the high solubility of complex **3** in pentane. **1H NMR (400 MHz, C6D6, 298 K):** δ = 9.92 (d, $^{3}J_{H,H}$ = 5.6 Hz, 1H; bpy), 8.92 (d, $^{3}J_{H,H}$ = 5.7 Hz, 1H; bpy), 7.75 (m, 4H; PPh_2), 7.50 (m, 4H; PPh_2), 7.25 (d, $^{3}J_{H,H}$ = 8.3 Hz, 1H; bpy), 7.09 (d, $^{3}J_{H,H}$ = 8.1 Hz, 1H; bpy), 7.02 (s, 1H; Mes), 7.00–6.76 (m, 15H; Ar), 6.60 (m, 2H; Ar), 3.24 (s, 3H; Mes), 2.47 (s, 3H; Mes), 2.24 (s, 3H; Mes). **$^{13}C\{^{1}H\}$ NMR (100 MHz, C_6D_6, 298 K):** δ = 152.39, 150.10, 142.15 (m), 140.62 (m), 135.89, 134.18, 129.82, 129.20, 128.60, 127.34, 123.47, 122.49, 121.32, 120.69, 26.40, 22.90 (br), 21.44. **$^{31}P\{^{1}H\}$ NMR (161.9 MHz, C_6D_6, 298 K):** δ = −20.9 (br). **$^{11}B\{^{1}H\}$ NMR (128 MHz, C_6D_6, 298 K):** δ = −7.68 (br). **Anal. calcd** for $C_{43}H_{39}BN_2NiP_2$ (714.20): C, 72.21; H, 5.50; N, 3.92. Found: C, 70.19; H, 5.50; N, 3.74.

[η³-*P,B,P*-$(PPh_2)_2$BMes]Ni$(CNXyl)_2$ (4)

In the glovebox, **2** (15 mg, 0.015 mmol) and 2,6-dimethylphenylisocyanide (5.9 mg, 0.030 mmol) were added to a 20 mL vial equipped with a stir bar. Approximately 2 mL of benzene was added and the resulting orange/green solution was allowed to stir for 30 min at 25 °C. The solvent was removed *in vacuo* and the resulting brown solid was washed with pentane to afford a brown solid (9.2 mg, 50%). This compound is unstable in solution ($t_{1/2}$ = 60 min) providing a mixture of as yet unidentified species including a broad resonance at δ_B = 31.2 ppm for the boroxin, $(MesBO)_3$[26] for which ^{1}H NMR (400 MHz, C_6D_6, 298 K) δ = 6.67 (s, 2H), 2.49 (s, 6H), 2.14 (3H). **^{1}H NMR (400 MHz, C_6D_6, 298 K):** δ = 7.77 (m, 4H; PPh_2), 7.72 (m, 4H; PPh_2), 7.07–6.68 (m, 20H; Ar), 2.98 (s, 3H; Mes), 2.45 (s, 3H; Mes), 2.30 (s, 6H; CNXyl), 2.23 (s, 6H; CNXyl), 2.11 (s, 3H; Mes). **$^{13}C\{^{1}H\}$ NMR (100 MHz, C_6D_6, 298 K):** δ = 141.98, 141.67, 137.81, 137.47, 137.13, 136.70 (t, $J_{C,P}$ = 6.2 Hz), 135.01, 134.73, 134.26, 134.01 (t, $J_{C,P}$ = 6.0 Hz), 128.81, 128.76, 128.59, 126.96, 126.88, 125.84, 28.38, 26.62, 25.63, 19.13, 19.10. **$^{31}P\{^{1}H\}$ NMR (161.9 MHz, C_6D_6, 298 K):** δ = −8.5. **$^{11}B\{^{1}H\}$ NMR (128 MHz, C_6D_6, 298 K):** δ = 4.75 (br). **FT-IR ATR (neat solid, cm^{-1}):** 2078, 2039, 1993 (br, ν(*CN*)). Appropriate elemental analysis could not be obtained for complex **4** due to decomposition.

[η³-*P,B,P*-$(PPh_2)_2$BMes]Ni(η²-C_2Ph_2) (5)

In the glovebox, **2** (21 mg, 0.031 mmol) and diphenylacetylene (5.5 mg, 0.031 mmol) were added to a 20 mL vial equipped with a stir bar. Approximately 2 mL of benzene was added and the orange solution was allowed to stir for 2 days at 25 °C. The solvent was removed *in vacuo* and the resulting orange solid was washed with pentane to afford an orange solid. Recrystallization from Et_2O or pentane at −35 °C gave orange crystals (16 mg, 70%). **^{1}H NMR (400 MHz, C_6D_6, 298 K):** δ = 8.17 (d, $^{3}J_{H,H}$ = 7.1 Hz, 4H; Ph_2C_2), 7.52 (m, 4H; PPh_2), 7.47 (m, 4H; PPh_2), 7.13 (t, $^{3}J_{H,H}$ = 7.5 Hz, 6H; Ar), 7.03 (t, $^{3}J_{H,H}$ = 7.4 Hz, 2H; Ar), 6.84 (m, 6H), 6.74 (m, 2H), 6.59 (t, $^{3}J_{H,H}$ = 7.6 Hz, 4H; Ar), 2.85 (s, 3H; Mes), 2.60 (s, 3H; Mes), 2.08 (s, 3H; Mes). **$^{13}C\{^{1}H\}$ NMR (100 MHz, C_6D_6, 298 K):** δ = 141.31, 140.49, 136.51, 136.35 (t, $J_{C,P}$ = 6.2 Hz), 133.07, 133.86 (m), 133.51 (m), 133.36 (t, $J_{C,P}$ = 6.0 Hz), 131.07, 128.99, 128.82, 128.74, 128.56, 128.42, 128.21, 127.94, 127.39, 25.78, 25.03, 21.26. **$^{31}P\{^{1}H\}$ NMR (161.9 MHz, C_6D_6, 298 K):** δ = −8.1. **$^{11}B\{^{1}H\}$ NMR (128 MHz,**

C_6D_6, 298 K): δ = 6.67 (br). **FT-IR ATR (neat solid, cm^{-1}):** 1823 (ν(CC)). **Anal. calcd** for $C_{47}H_{41}BNiP_2$ (736.21): C, 76.57; H, 5.61. Found: C, 74.29; H, 5.76.

[η³-*P,B,P*-$(PPh_2)_2$BMes]Pt$(CH_3)_2$ (6)

In the glovebox, **1** (60 mg, 0.12 mmol) and $Pt(Me)_2(COD)$ (40 mg, 0.12 mmol) were added to a 20 mL vial equipped with a stir bar. Approximately 2 mL of benzene was added and the orange solution was allowed to stir for 4 days at 25 °C. The solvent was removed *in vacuo* and the resulting yellow solid was recrystallized from saturated Et_2O at −35 °C to give yellow crystals (77 mg, 88%). N.B. Heating this reaction mixture results in decomposition to Pt(0) and undesired organic by-products. **^{1}H NMR (400 MHz, C_6D_6, 298 K):** δ = 7.47 (m, 4H; PPh_2), 7.42 (m, 4H; PPh_2), 6.81 (m, 8H; PPh_2), 6.72 (s, 1H; Mes), 6.66 (s, 1H; Mes), 6.62 (t, $^3J_{H,H}$ = 7.6 Hz, 4H; PPh_2), 2.81 (s, 3H; Mes), 2.78 (s, 3H; Mes), 2.17 (s with ^{195}Pt satellites, $^3J_{H,Pt}$ = 80 Hz, 6H; Pt–C$\underline{H}_3$), 2.06 (s, 3H; Mes). **^{13}C{^{1}H} NMR (100 MHz, C_6D_6, 298 K):** δ = 142.64, 140.08, 136.30 (t, $J_{C,P}$ = 5.1 Hz), 133.60 (t, $J_{C,P}$ = 4.8 Hz), 129.74, 129.62, 129.41, 128.82, 128.54 (t, $J_{C,P}$ = 6.1 Hz), 128.24 (t, $J_{C,P}$ = 6.0 Hz), 124.75 (t, J = 33 Hz), 25.50, 25.45, 21.21, 4.52 (t with ^{195}Pt satellites, $J_{C,Pt}$ = 688 Hz, $J_{C,P}$ = 27.8 Hz; Pt–$\underline{C}H_3$). **^{31}P{^{1}H} NMR (161.9 MHz, CD_2Cl_2, 298 K):** δ = −21.6 (br t, $^1J_{Pt,P}$ = 853 Hz). **^{11}B{^{1}H} NMR (128 MHz, CD_2Cl_2, 298 K):** δ = +7.9 (br). **Anal. calcd** for $C_{35}H_{37}BP_2Pt$ (725.21): C, 57.94; H, 5.14. Found: C, 59.23; H, 5.08.

Pt[κ²-*P,P*-$(PPh_2)_2$B(Mes)(I)][κ²-P,P-$(PPh_2)_2$B(Mes)(CH_3)] (10)

In the glovebox, **1** (30 mg, 0.12 mmol, 2 equiv.) and $[Pt(Me)_3(I)]_4$ (11 mg, 0.03 mmol, 0.25 equiv.) were added to a 20 mL vial equipped with a stir bar. Approximately 2 mL of benzene was added and the colorless solution was allowed to stir for 4 days at 25 °C. The solvent was removed *in vacuo* and the resulting pale yellow solid was recrystallized from saturated Et_2O at −35 °C to give clear colorless crystals (14 mg, 38%). **^{1}H NMR (400 MHz, C_6D_6, 298 K):** δ = 7.92 (br; 4H PPh_2), 7.77 (br, 4H; PPh_2), 7.05 (br, 12H; PPh_2), 6.92 (t, $^3J_{H,H}$ = 7.6 Hz, 4H; PPh_2), 6.82 (t, $^3J_{H,H}$ = 7.6 Hz, 4H; PPh_2), 6.77 (s, 2H; Mes), 6.75 (t, $^3J_{H,H}$ = 7.6 Hz, 4H; PPh_2), 6.69 (s, 2H; Mes), 6.63 (t, $^3J_{H,H}$ = 7.6 Hz, 4H; PPh_2), 6.56 (t, $^3J_{H,H}$ = 7.6 Hz, 4H; PPh_2), 2.23 (s, 6H; Mes), 2.15 (s, 9H (6H + 3H); Mes), 2.08 (s, 3H; Mes), 1.45 (t, $^3J_{H,P}$ = 19.4 Hz, 3H; B–C$\underline{H}$)$_3$. **^{13}C{^{1}H} NMR (100 MHz, THF-d_8, 298 K):** δ = 142.08 (m), 140.85 (m), 137.07 (m), 136.44, 136.25 (m), 135.91 (m), 134.90 (m), 134.35, 133.26, 132.07, 130.90, 129.87, 129.68 (m), 129.30 (m), 128.85, 128.61 (m), 128.41, 128.25, 127.99, 127.25, 26.64, 26.26, 20.56, 20.55, 8.66 (br, B–$\underline{C}H_3$). **^{31}P{^{1} H} NMR (161.9 MHz, C_6D_6, 298 K):** δ = −35.65 (m). **^{11}B{^{1}H} NMR (128 MHz, C_6D_6, 298 K):** δ = 4.94. **Anal. calcd** for $C_{67}H_{65}B_2IP_4Pt$ (1337.29): C, 60.16; H, 4.90. Found: C, 58.05; H, 4.96.

Supplementary Material

Refer to Web version on PubMed Central for supplementary material.

Acknowledgements

This work was supported by the NIH (GM070757), NSERC (Banting PDF award to MWD), and the Resnick Sustainability Institute at Caltech (Postdoctoral award to MWD). We thank Larry Henling and Mike Takase for assistance with X-ray crystallography.

References

1. Green MLH. J. Organomet. Chem. 1995; 500:127–148.
2. Jiang F, Shapiro PJ, Fahs F, Twamley B. Angew. Chem., Int. Ed. 2003; 42:2651–2653.
3. Kolpin KB, Emslie DJH. Angew. Chem., Int. Ed. 2010; 49:2716–2719.
4. Nesbit MA, Suess DLM, Peters JC. Organometallics. 2015; 34:4741–4752.
5. Macmillan SN, Harman WH, Peters JC. Chem. Sci. 2014; 5:590–597.
6. Emslie DJH, Cowie BE, Kolpin KB. Dalton Trans. 2012; 41:1101–1117. [PubMed: 21983808]
7. Kaufmann B, Nöth H, Paine RT, Polborn K, Thomann M. Angew. Chem., Int. Ed. 2003; 32:1446–1448.
8. Amgoune A, Ladeira S, Miqueu K, Bourissou D. J. Am. Chem. Soc. 2012; 134:6560–6563. [PubMed: 22480251]
9. Bartlett RA, Dias H, Power PP. Inorg. Chem. 1988; 27:3919–3922.
10. Langer J, Görls H, Gillies G, Walther D. Z. Anorg. Allg. Chem. 2005; 631:2719–2726.
11. Scarborough CC, Wieghardt K. Inorg. Chem. 2011; 50:9773–9793. [PubMed: 21678919]
12. Waterman R, Hillhouse GL. Organometallics. 2003; 22:5182–5184.
13. Kakeya M, Tanabe M, Nakamura Y, Osakada K. J. Organomet. Chem. 2009; 694:2270–2278.
14. Figueroa JS, Melnick JG, Parkin G. Inorg. Chem. 2006; 45:7056–7058. [PubMed: 16933903]
15. Bouhadir G, Bourissou D. Chem. Soc. Rev. 2016; 45:1065–1079. [PubMed: 26567634]
16. Schindler T, Lux M, Peters M, Scharf LT, Osseili H, Maron L, Tauchert ME. Organometallics. 2015; 34:1978–1984.
17. Cowie BE, Emslie DJH. Organometallics. 2015; 34:2737–2746.
18. Braunschweig H, Dewhurst RD, Schneider A. Chem. Rev. 2010; 110:3924–3957. [PubMed: 20235583]
19. Khusnutdinova JR, Milstein D. Angew. Chem., Int. Ed. 2015; 54:12236–12273.
20. Sircoglou M, Bouhadir G, Saffon N, Miqueu K, Bourissou D. Organometallics. 2008; 27:1675–1678.
21. Devillard M, Nicolas E, Appelt C, Backs J, Mallet-Ladeira S, Bouhadir G, Slootweg JC, Uhl W, Bourissou D. Chem. Commun. 2014; 50:14805–14808.
22. Fischbach A, Bazinet PR, Waterman R, Tilley TD. Organometallics. 2008; 27:1135–1139.
23. Thibault M-H, Boudreau J, Mathiotte S, Drouin F, Sigouin O, Michaud A, Fontaine F-G. Organometallics. 2007; 26:3807–3815.
24. Boudreau J, Fontaine F-G. Organometallics. 2011; 30:511–519.
25. Yang L, Powell DR, Houser RP. Dalton Trans. 2007; 60:955–964.
26. Cole SC, Coles MP, Hitchcock PB. Dalton Trans. 2003:3663.

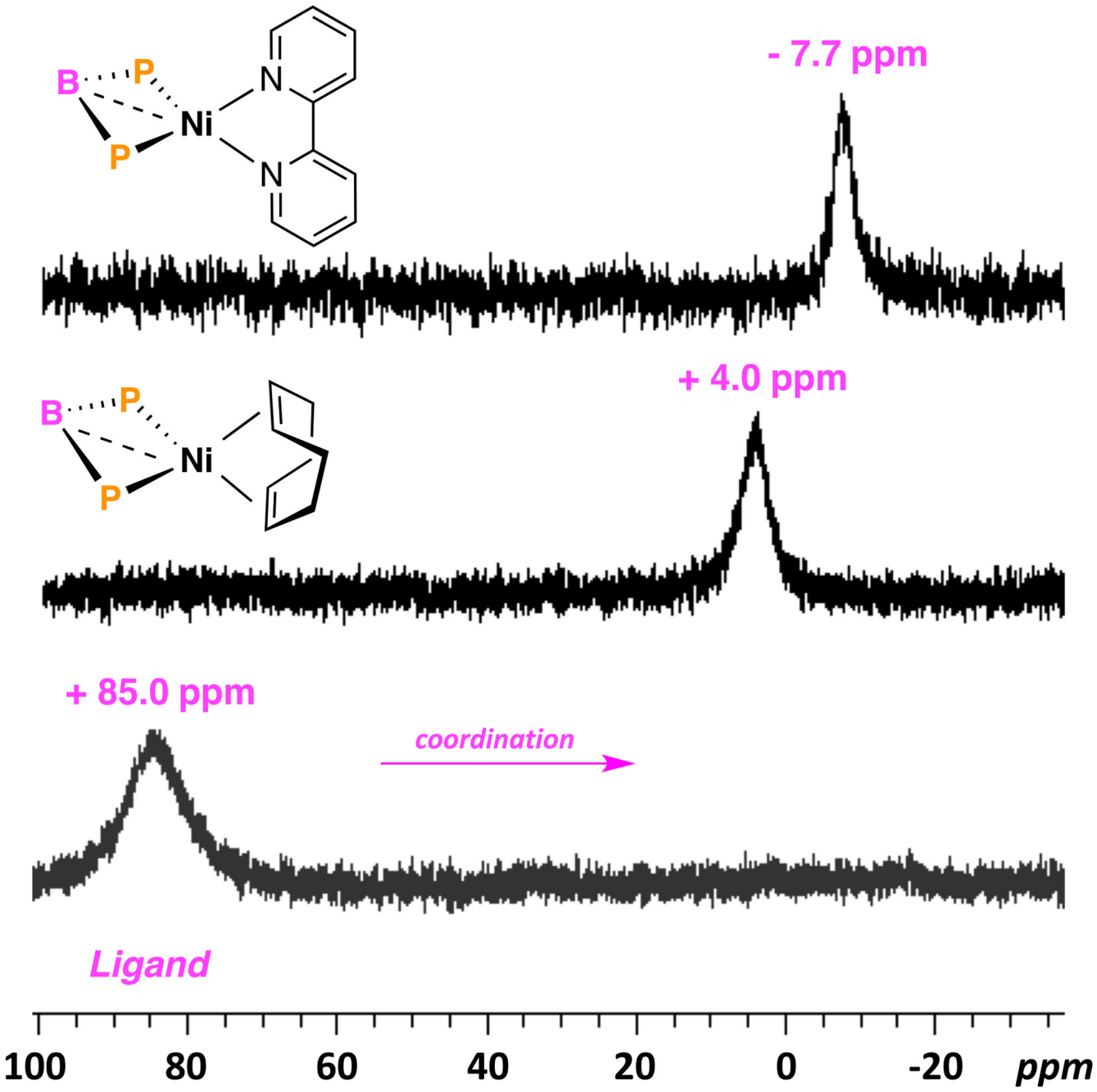

Fig. 1.
$^{11}B\{^{1}H\}$ NMR spectra of ligand 1 and complexes **2** and **3** (128 MHz, C_6D_6, 298 K).

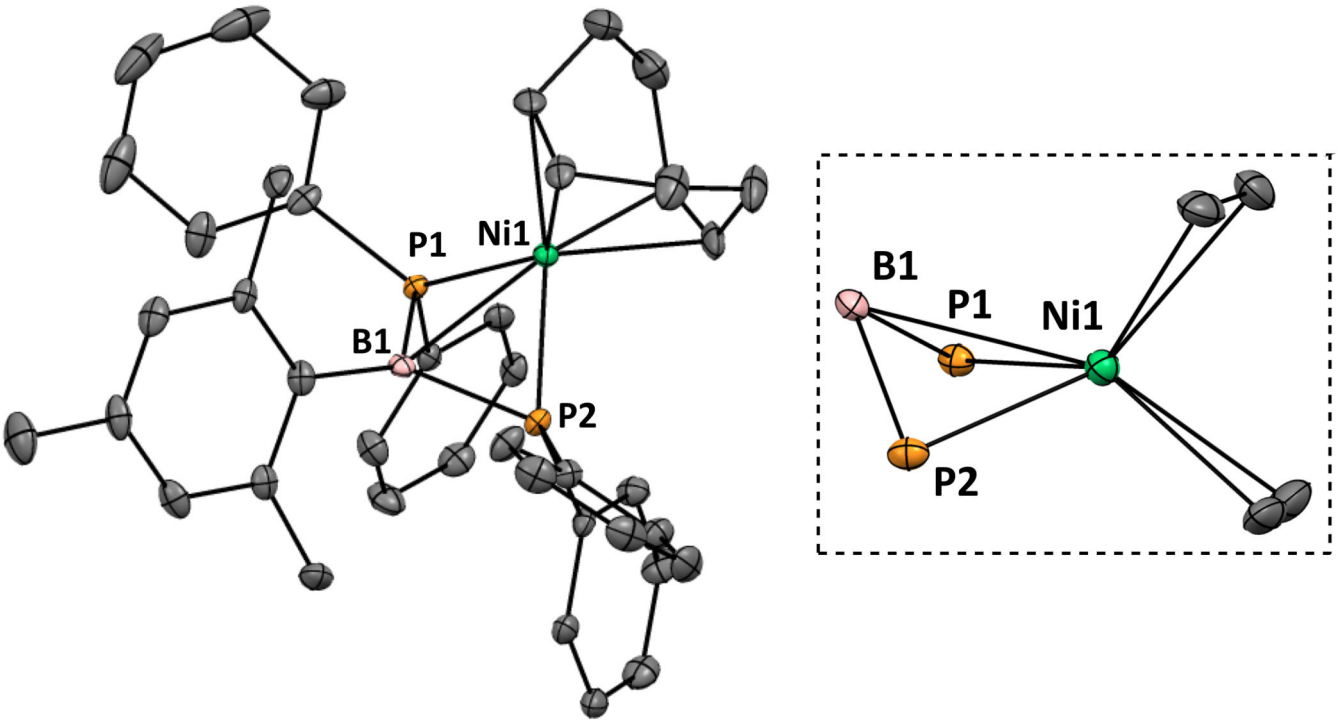

Fig. 2.

ORTEP depiction of the solid-state molecular structure of 2 (displacement ellipsoids are shown at the 50% probability, hydrogens omitted for clarity). Selected bond lengths [Å] and angles (°). Ni(1)–P(1) 2.183(1), Ni(1)–P(2) 2.190(1), Ni(1)–B(1) 2.329(4), P(1)–Ni(1)–P(2) 85.46(4), P(1)–B(1)–P(2) 102.8(2).

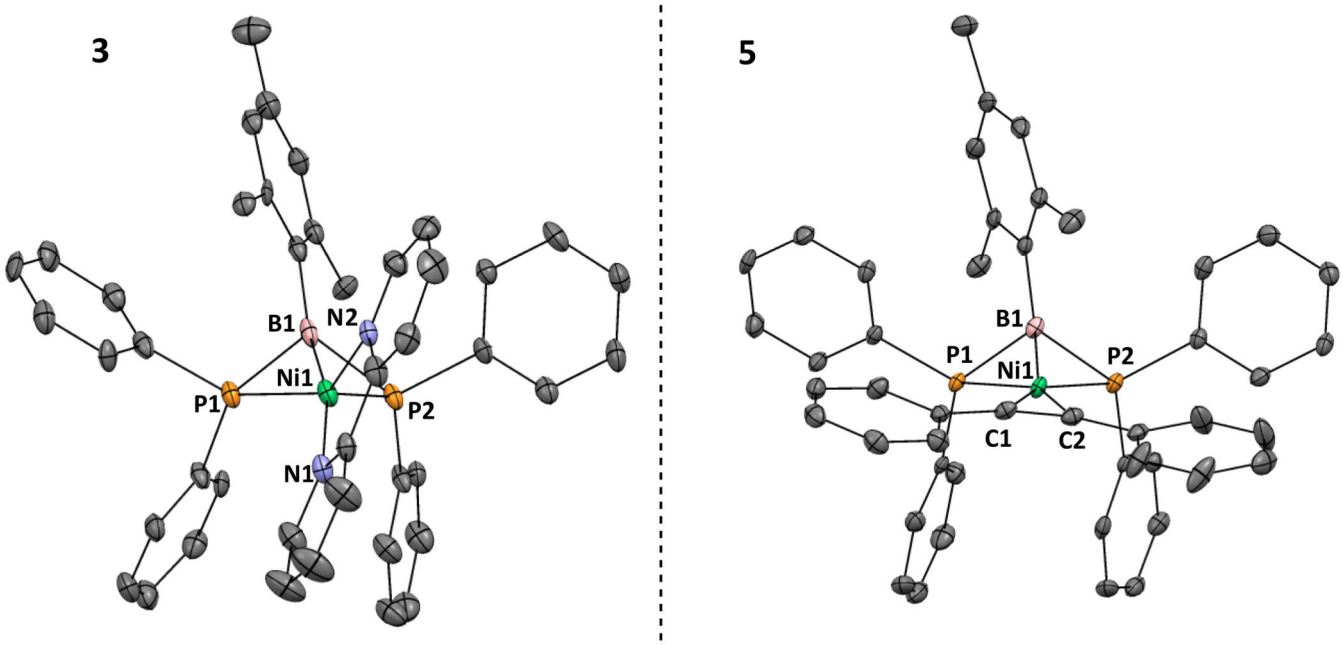

Fig. 3.

ORTEP depiction of the solid-state molecular structure of 3 and 5 (displacement ellipsoids are shown at the 50% probability, hydrogens omitted for clarity).

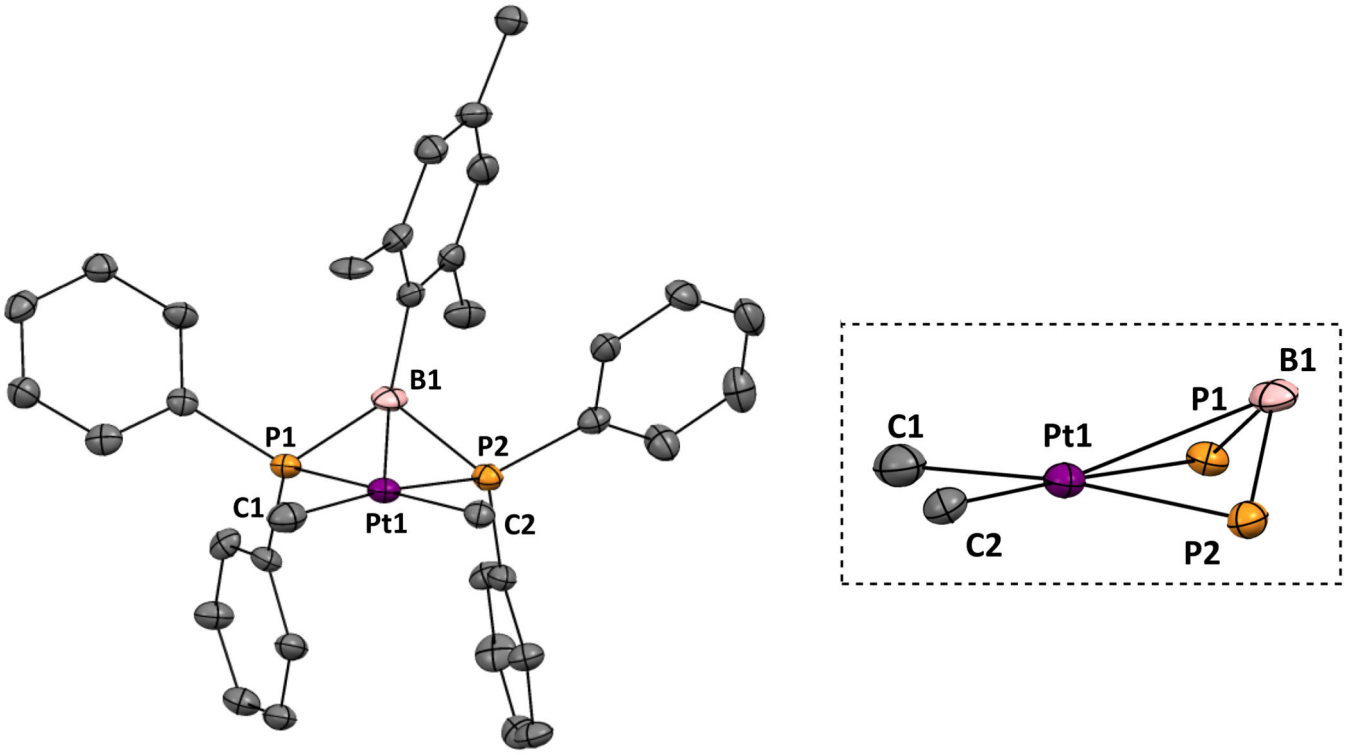

Fig. 4.

ORTEP depiction of the solid-state molecular structure of 6 (displacement ellipsoids are shown at the 50% probability, hydrogens omitted for clarity). Selected bond lengths [Å] and angles (°). Pt(1)–P(1) 2.305(3), Pt(1)–P(2) 2.318(2), Pt(1)–B(1) 2.403(11), Pt(1)–C(1) 2.093(9), Pt(1)–C(2) 2.103(12), P(1)–Pt(1)–P(2) 81.08(9), P(1)–B(1)–P(2) 106.9(5).

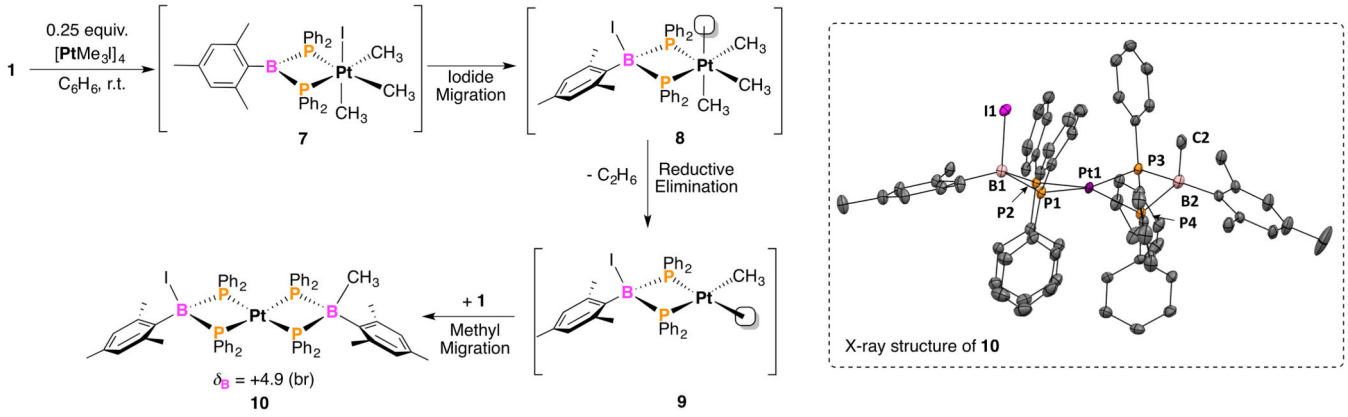

Fig. 5.

Generation of complex **10** and ORTEP depiction of the solid-state molecular structure of 10 (displacement ellipsoids are shown at the 50% probability, hydrogens omitted for clarity).

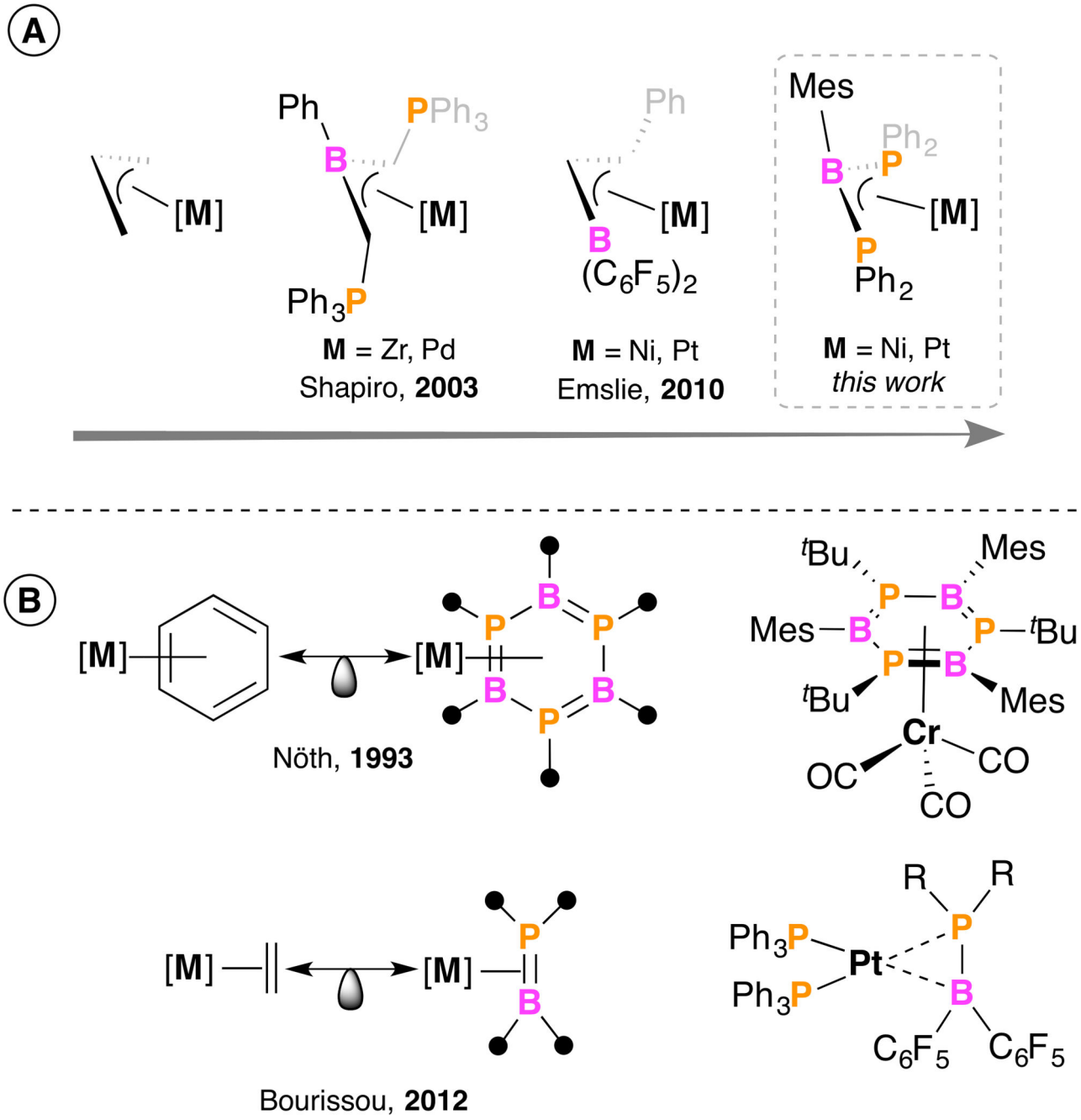

Chart 1.
Overview of boron-based ligand platforms.

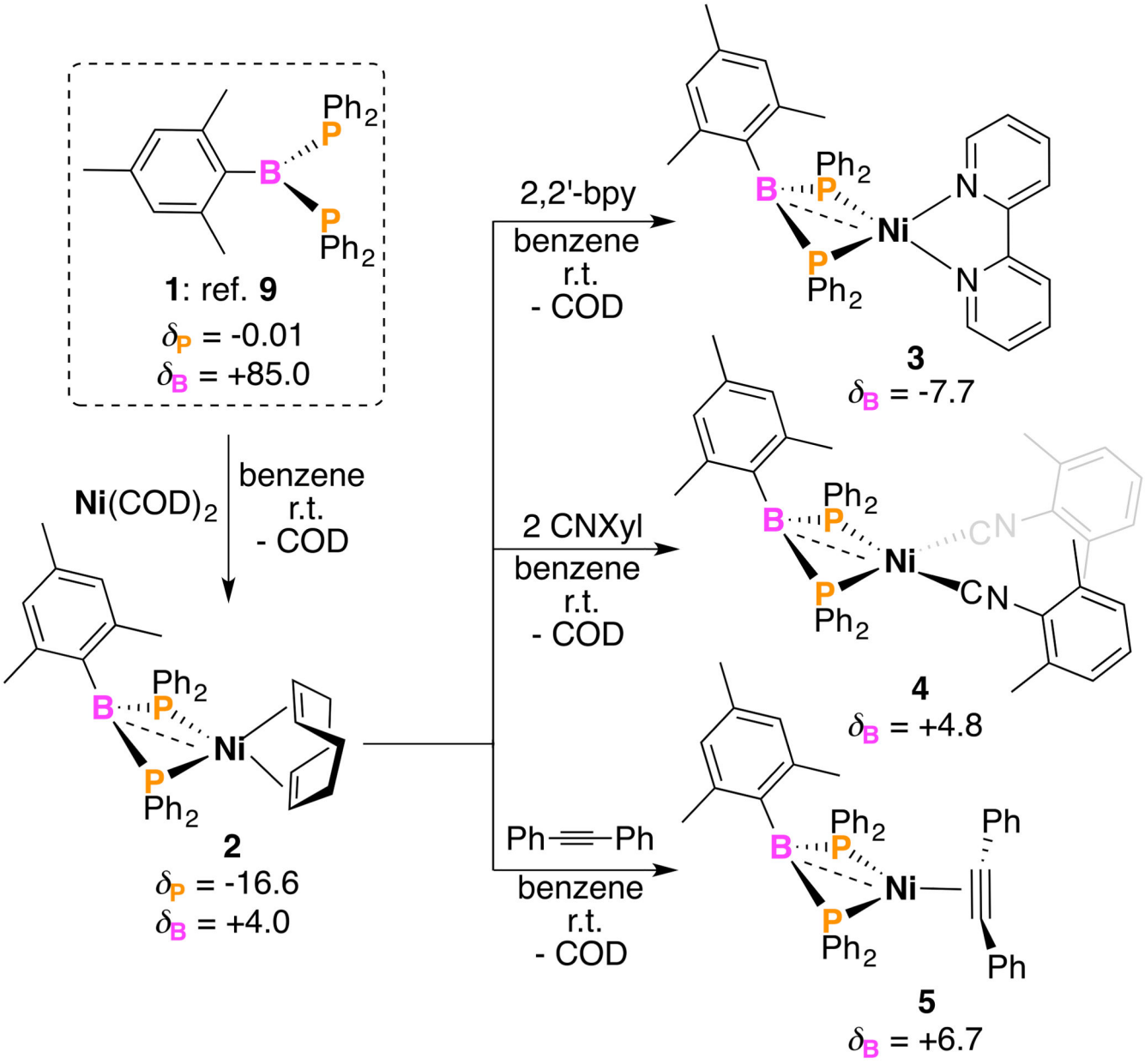

Scheme 1.
Generation of η^3-*P,B,P*-$(PPh_2)_2$BMes Ni complexes.

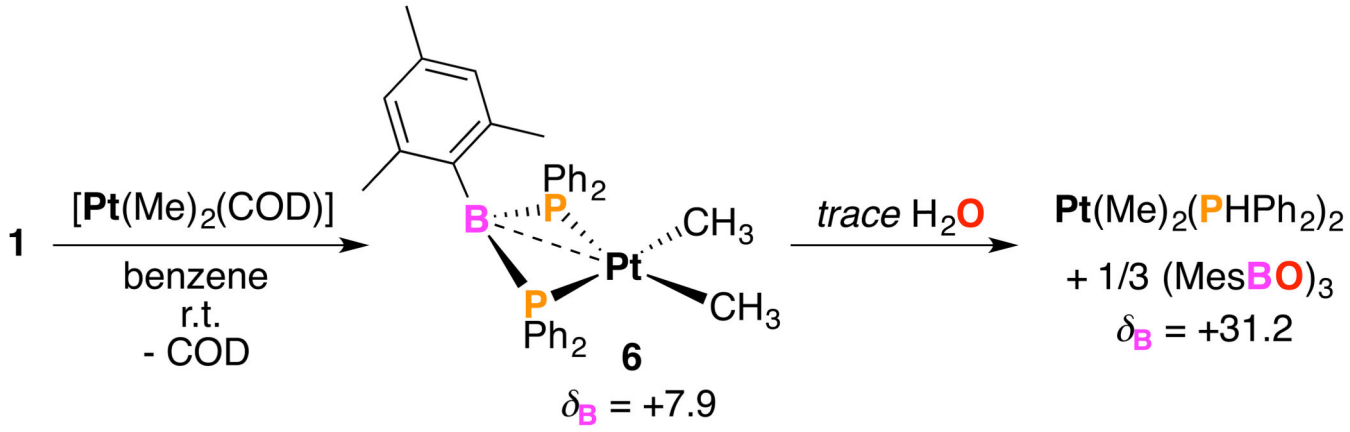

Scheme 2.
Generation of η^3-*P,B,P*-$(PPh_2)_2$BMes Pt^{II} complex **6**.